Improved perturb and observation maximum power point tracking technique for solar photovoltaic power generation systems

Manoharan, Premkumar; Subramaniam, Umashankar; Babu, Thanikanti Sudhakar; Padmanaban, Sanjeevikumar; Holm-Nielsen, Jens Bo; Mitolo, Massimo; Ravichandran, Sowmya

Published in:
IEEE Systems Journal

DOI (link to publication from Publisher):
10.1109/JSYST.2020.3003255

Publication date:
2021

Document Version
Accepted author manuscript, peer reviewed version

Improved Perturb and Observation Maximum Power Point Tracking Technique for Solar Photovoltaic Power Generation Systems

Premkumar Manoharan, Umashankar Subramaniam, *Senior Member, IEEE*, Thanikanti Sudhakar Babu, *Member, IEEE*, Sanjeevikumar Padmanaban, *Senior Member, IEEE*, Jens Bo Holm-Nielsen, Massimo Mitolo, *Fellow, IEEE*, and Sowmya Ravichandran

***Abstract*—The primary concerns in the practical photovoltaic (PV) system are the power reduction due to the change in operating conditions, such as the temperature or irradiance, the high computation burden due to the modern maximum power point tracking (MPPT) mechanisms, and to maximize the PV array output during the rapid change in weather conditions. The conventional perturb and observation (P&O) technique is preferred in most of the PV systems. Nevertheless, it undergoes false tracking of maximum power point (MPP) during the rapid change in solar insolation due to the wrong decision in the duty cycle. To avoid the computational burden and drift effect, this article presents a simple and enhanced P&O MPPT technique. The proposed technique is enhanced by including the change in current (*dI*), in addition to the changes in output voltage and output power of the PV module. The effect of including the *dI* profile with the traditional method is explained with the fixed and variable step-size methods. The mathematical expression for the drift-free condition is derived. The traditional boost converter is considered for validating the effectiveness of the proposed methods by employing the direct duty cycle technique. The proposed algorithm is simulated using MATLAB/Simulink and validated under various scenarios with the developed laboratory prototype in terms of drift-free characteristics and tracking efficiency. The result proves that the proposed technique can track the MPP accurately under various operating conditions.**

***Index Terms*—Adaptive perturb and observation (P&O), boost converter, change in current, direct duty cycle control, drift effect, maximum power point tracking (MPPT).**

Manuscript received February 1, 2020; revised April 12, 2020; accepted May 21, 2020. *(Corresponding author: Sanjeevikumar Padmanaban.)*

Premkumar Manoharan is with the Department of Electrical and Electronics Engineering, GMR Institute of Technology, Rajam 532127, India (e-mail: premkumar.m@gmrit.edu.in).

Umashankar Subramaniam is with Renewable Energy Laboratory, Prince Sultan University, Riyadh 11461, Saudi Arabia (e-mail: usubramaniam@psu.edu.sa).

Thanikanti Sudhakar Babu is with the Department of Electrical Power Engineering, Universiti Tenaga Nasional, Kajang 43000, Malaysia (e-mail: sudhakarbabu66@gmail.com).

Sanjeevikumar Padmanaban and Jens Bo Holm-Nielsen are with the Center for Bioenergy & Green Engineering Department of Energy Technology, Aalborg University, 6700 Esbjerg, Denmark (e-mail: sanjeevi_12@yahoo.co.in; jhn@et.aau.dk).

Massimo Mitolo is with the School of Integrated Design, Engineering and Automation, Irvine Valley College, Irvine, CA 92602 USA (e-mail: mmitolo@ivc.edu).

Sowmya Ravichandran is with the Department of Electrical and Electronics Engineering, National Institute of Technology, Tiruchirapalli 620001, India (e-mail: sowmyanitt@gmail.com).

Digital Object Identifier 10.1109/JSYST.2020.3003255

NOMENCLATURE

$\eta_{\text{converter}}$	Converter efficiency in %.
V_{pv} and V_0	PV voltage and converter output voltage in V.
V_{oc}	Open-circuit voltage of the PV module in V.
I_{pv} and I_0	PV current and converter output current in A.
I_{sc}	Short-circuit current of the PV module in A.
$I_{\text{sc},n}$	Nominal short-circuit current in A.
I_o	Diode saturation current in A.
R_{in} and R_0	Input resistance and load resistance in Ω.
R_{se} and R_p	Series and shunt resistance of the panel in Ω.
D	Duty cycle of converter MOSFET switch.
dV and dI	Change in voltage in V and current in A.
dP	Change in power in Watt.
dD	Perturbation size constraint.
T_p	Perturbation time in seconds.
M	Scaling factor.
a	Ideality factor of the diode.
V_T	Thermal voltage.
G and G_n	Actual and nominal solar irradiation in W/m^2.
dG	Change in solar irradiation in W/m^2.
K_I	Temperature coefficient.
T and T_n	Actual and nominal temperature in K.
dT	Difference between T and T_n in K.
f_s	Switching frequency in kHz.
L	Inductance of the boost converter in mH.
C_{in} and C_{out}	Input and output capacitors in μF, respectively.

I. INTRODUCTION

SOLAR photovoltaic (PV) power generation has long been seen as a clean and green energy, and it has advantages such as being ecofriendly, noise-free, and low maintenance. Nevertheless, the PV characteristics are nonlinear, and it is a challenging issue to operate at the maximum power point (MPP) to produce maximum possible output power [1]. Therefore, the solar PV panel characteristics, such as current (*I*)-voltage (*V*) and power (*P*)–*V* characteristics, get altered when solar insolation and the cell temperature change. Therefore, it is essential to track the MPP from the profile of the PV panel. The maximum output power from the PV module is extracted using MPPT techniques, and a power electronic-based converter plays an essential role in it. Therefore, the MPP can be tracked by adjusting the duty cycle of the power electronics converter. Various types of converters, e.g., boost, buck, buck–boost, interleaved converter, and SEPIC converter, are considered in the literature. Each PV system is

TABLE I
SUMMARY OF ADVANTAGES AND DISADVANTAGES OF A FEW MPPT METHODS

Type	Name of the method	Advantages	Drawbacks
Traditional Methods	Incremental conductance [5], P&O [5], Incremental resistance [6], Hill-climbing [7], and Fractional open circuit voltage/short circuit current [8]	Easy to implement, simple structure, and low-cost	Steady-state oscillation, no guarantee for convergence, drift problem, reduced efficiency, and frequent tuning of specific parameters.
Modern Methods	Fuzzy logic control [9], Grey wolf optimization [10], Sliding mode control [11], Cuckoo search (CS) [12], deterministic CS [13], Ant colony optimization (ACO) [14], Particle swarm optimization (PSO) [15], distributive PSO [16], and Artificial bee colony [17], shade-tolerant [18], and demand response multi-objective model [19]	Robust, no steady-state and transient oscillations, high tracking efficiency, and few parameters requires tuning	Large search space, computational complexity, high cost, and hardware implementation
Hybrid methods	P&O-PSO [20-21], P&O-humpback whale [22], variants of Flower pollination algorithm [23-24], P&O-ACO [25], Exchange market-Genetic algorithm [26], and Adaptive neuro-fuzzy inference system-PSO [27]	Higher tracking accuracy reduced power oscillation, and tracking efficiency is higher than 98%	High cost, difficult to control, steep in hardware implementation, and convergence is assured if the global peak is situated outside the search zone

provided with the MPPT controller as an essential part [2]–[4]. There are numerous techniques introduced by many researchers to increase the tracking accuracy and efficiency of solar power generation systems. Table I summarizes the advantages and disadvantages of various MPPT techniques. However, none of the above methods is perfect, since few methods have good tracking accuracy with poor steady-state performance; few methods have less steady-state oscillations with high computation burden; or few other having good steady-state and dynamic responses. Nevertheless, it is highly dependent on the designer.

Even now, the authors are still reporting bio-inspired algorithm based MPPT methods and claiming that it gives better results. However, the solar PV companies are not ready to employ these methods due to their complexity in developing controller board which should synchronize with the speed of the algorithm. To incorporate this, it involves high-cost devices, such as controllers, and its development is still under process. Therefore, it is observed from the literature that the conventional algorithms are the most preferred in real-time applications and commercialized algorithms for solar photovoltaic applications. With this inspiration, in this article, authors focused on the traditional perturb and observation (P&O) technique due to its advantages, such as it can be used in digital and analogue platforms, free from frequent tuning, independent of the PV array, and ease of implementation. The working principle of the traditional technique is based on the dP/dV slope from the P–V curve of the panel. The operating voltage is perturbed depending on the nature of the slope to track the MPP. The P&O MPPT technique is implemented by using reference voltage control or DDC along with the proportional-integral controller, as discussed in various literature works [28]. The success of the traditional P&O method is analyzed by measuring oscillations in power and the tracking time. The power oscillation and tracking time depend on the perturbation size. The power oscillations are reduced by selecting a small perturbation size though it increases the settling time. Moreover, the traditional P&O technique is unsuccessful in tracking the MPP accurately under sudden variations in solar insolation and temperature, and the same effect has been analyzed in various literature [29].

The conventional P&O technique suffers from three main drawbacks. First, the P&O technique is likely to lose its tracking path, i.e., drift issue, during a rapid change in solar irradiance. Once the path is incorrect, the algorithm deviates away from the MPP due to which energy loss might increase. Second, the P&O is not capable of tracking the global peak (GP) under various shading conditions. Third, the nature of the algorithm that forces the operating point to oscillate around the MPP. Due to this, the power loss is increased. To improve the performance of the conventional P&O method, many researchers reported adaptive step-size based techniques [30], [31]. But, the success rate in tracking the MPP during shading conditions depends on the scaling factor decided by the researcher and requires frequent on-line tuning of specific parameters [32], [33].

On the other hand, an enhanced P&O technique that can handle partial shading conditions is presented in [34] and [35]. However, the technique completely ignores the drift problem, and therefore, the solutions delivered by the earlier papers do not handle all the key issues at the same time. Table II summarizes other enhanced P&O techniques. Even though the P&O and adaptive P&O are successfully implemented, the drift issue for a rapid change in insolation remains unsolved. Furthermore, with this motivation, this article presents an enhanced P&O method to reduce the failure in tracking MPP during a fast change in insolation and one-time insolation change. By applying the perturbation size constraint (dD), this problem can be reduced. To avoid failure during a rapid change in insolation, a large step size can be selected. However, it increases the steady-state power oscillations and also the power loss. As per the observations from some of the presented literature, this problem can also be reduced by setting up the lower and upper dP limits. However, this is not an optimal solution because the value of dP is mainly dependent on the change in solar insolation.

In this article, the authors proposed an easy and accurate MPPT technique to avoid failure in tracking the MPP under a fast change in solar insolation. The divergence problem and the steady-state power oscillation are reduced by considering the change in output current (dI) profile along with the traditional P&O MPPT technique. The proposed modified P&O technique is tested with both fixed step size and variable step size. To implement this technique, the dc–dc converter is required between the load and the PV module. Thus, in this article, the traditional boost converter is selected and effectively designed as per the system ratings to meet the objectives of the MPPT.

The remaining sections of the article are arranged as follows. Section II describes the solar PV characteristics under uniform and nonuniform irradiation conditions. The problems and findings of the conventional P&O algorithm are discussed in Section III. The proposed MPPT technique is modeled and analyzed in Section IV. The simulation results under different operating conditions are given in Section V. The experimental

TABLE II
SUMMARY OF VARIOUS ENHANCED P&O MPPT METHODS

Ref.	Type of perturbation/Control variable	Complexity	Convergence speed	Tracking efficiency under a rapid change in insolation
[29]	Dynamic perturbation/Duty ratio	High	Medium	Low
[30]	Dynamic perturbation/Voltage	Medium	Medium	Medium
[33]	Dynamic perturbation/Duty ratio	High	Low	Low
[34]	Dynamic perturbation/Duty ratio	Medium	High	High
[35]	Dynamic perturbation/Duty ratio	Medium	High	Medium

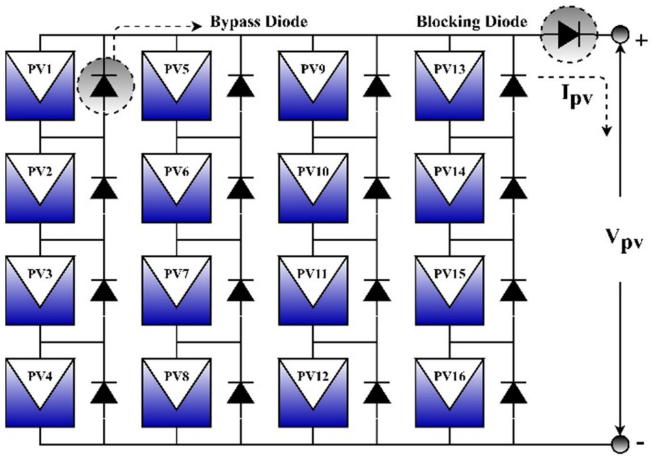

Fig. 1. Simple structure of the PV array.

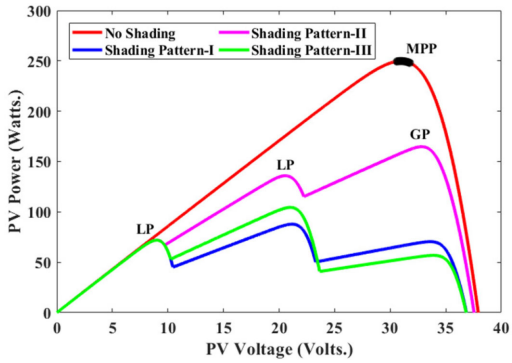

Fig. 2. *P–V* characteristics in uniform and nonuniform operating conditions of the PV array.

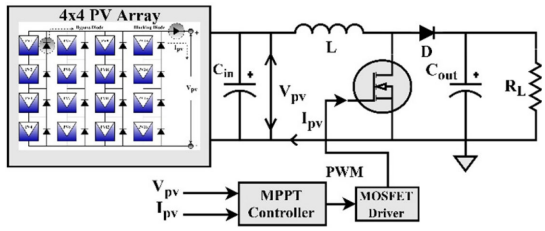

Fig. 3. Block diagram of the PV power system.

validation under different scenarios is presented in Section VI. Section VII concludes the article.

II. PV ARRAY CHARACTERISTICS UNDER DIFFERENT OPERATING SCENARIOS

The solar PV array is formed by connecting the PV modules in series and parallel combinations to acquire the required current and voltage rating. The sum of the individual power rating of the module is equal to the rating of the PV array. A simple PV array structure is displayed in Fig. 1. The PV array has four panels in a string, and four PV strings are attached in parallel (4×4).

If cells/panels are shaded due to various reasons, then the shaded cell/panel acts as a load instead of the source [36]. In due effect, the shaded panels will be damaged if the hotspot increases. To reduce the hotspots in the panel, the bypass diode is connected across each panel during shading conditions [37]. The reverse current to the PV module is restricted by connecting the blocking diode. During the unshaded/normal condition, the PV panel exhibits a single peak on *P–V* characteristic. On the other hand, during shaded conditions, the panel has multiple peaks, such as two or more local peaks (LPs) and one GP.

The same can be visualized in the *P–V* curve of the PV array, and the curves under different shading conditions are shown in Fig. 2. It is essential to drive the *PV* module at GP to generate the maximum output power, instead of operating at LP. So, it is essential to find an effective MPPT method to produce the maximum output power with good tracking time and accuracy [38], [39].

III. COMMON PROBLEMS OF TRADITIONAL P&O MPPT TECHNIQUE

The operating point of the PV panel mainly depends on the impedance mismatch between the load and the PV panel, and the dc–dc converter can resolve the problem by adjusting the duty ratio. Therefore, the explanation in this section starts with the traditional dc–dc boost converter and then extended to the traditional P&O MPPT algorithm. The block diagram of the overall PV system is shown in Fig. 3.

As discussed earlier, in MPPT control, the duty cycle of the switch has been adjusted. However, the reason behind this duty cycle control can be explained concerning the converter efficiency. The efficiency of the conventional boost converter ($\eta_{\text{Converter}}$) can be determined by making use of the relationship between the output voltage and input voltage, and the same has been presented in

$$\eta_{\text{Converter}} = \frac{V_0 \times I_0}{V_{\text{pv}_0} \times I_{\text{pv}}} = \frac{V_{00} \times I_0}{{V_{\text{pv}}}^2{}_0 \times R_{\text{in}}} = \frac{V_0^2}{V_{\text{pv}}^2} \frac{R_{\text{in}}}{R_0} \quad (1)$$

$$\eta_{\text{Converter}} = \left(\frac{1}{1-D}\right)^2 \frac{R_{\text{in}}}{R_0} \quad (2)$$

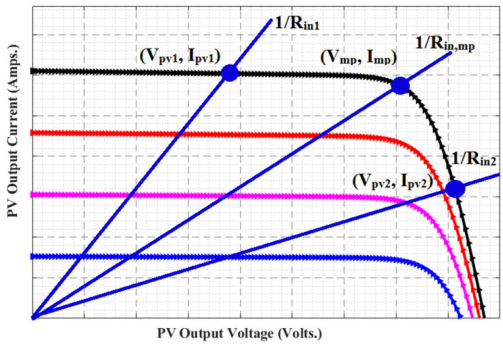

Fig. 4. Operating point variation concerning the load line.

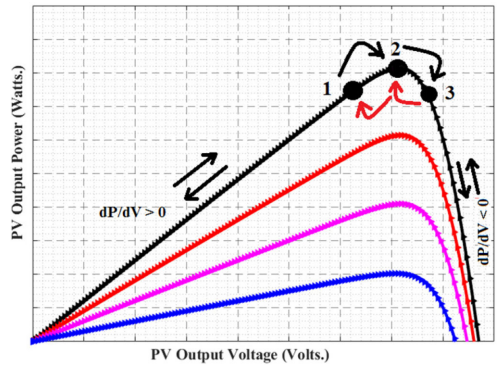

Fig. 5. Variation in slope and steady-state operation.

where $I_{\rm pv}$ and $V_{\rm pv}$ represent the PV current and the PV voltage, respectively, the converter input resistance can be determined as

$$R_{\rm in} = \eta_{\rm Converter} \times (1-D)^2 \times R_0. \tag{3}$$

It is observed from (3) that the operating point can be controlled by adjusting the converter duty cycle. Besides, the input resistance ($R_{\rm in}$) also varies, and the same can be understood from Fig. 4. The controller tracks the MPP by regulating the duty ratio of the converter.

As discussed earlier, the P&O method is established based on variation in the slope (*dP/dV*) on the *P–V* curve of the solar PV panel. It is observed from Fig. 5 that the slope is positive at the left-hand side of MPP and is negative at the right-hand side of MPP. The duty cycle is perturbed based on the slope polarity to track the MPP. In Fig. 5, points 1, 2, and 3 represent the operating point on the *P–V* characteristics during perturbation, and the arrow mark indicates that moment of operating point based on the polarity of the slope.

As discussed in various literature works, the voltage of the PV module and the converter duty cycle are inversely proportional. An increase in the converter duty cycle causes the PV output voltage to reduce and vice versa. There are two essential parameters in the conventional MPPT algorithms, such as perturbation size and perturbation time [28], [40]. Since these two parameters decide the convergence speed and accuracy of the P&O MPPT method, it is necessary to select the proper values. Therefore, the criteria for selecting the above-said parameters are discussed in the subsections.

A. Selection of Perturbation Time (Tp)

The time, T_p, should be less than the settling time of the converter to reduce the power oscillations in the conventional P&O technique for a change in duty ratio of the converter. The perturbation size (*dD*) and the settling time of the converter are directly proportional to each other. However, for an adaptive method, the perturbation time is larger than the settling time of the converter for a maximum variation in duty ratio ($dD_{\rm max}$).

B. Selection of Perturbation Size (dD)

By considering the performance under steady-state and transient state conditions, the perturbation size is selected. If the size of the perturbation is less, then the performance under steady-state is improved, whereas if the perturbation size is maximum, then the performance under the transient state is improved. The minimum step size can be selected based on the analog-digital converter resolution, microcontroller, and tracking accuracy of the system. Due to the switching ripple of the semiconductor on the PV voltage, the optimal perturbation size can be selected, such that the PV voltage deviation due to the size of the perturbation should be higher than the swell of PV output voltage. The performance of this conventional MPPT algorithm is analyzed by the drift occurrence, tracking efficiency, and steady-state response [41], [42].

C. Steady-State Behavior of P&O Algorithm

The process of the conventional P&O MPPT method under steady state is shown in Fig. 5. Consider that the operating point on the *P–V* curve has been relocated from point-1 to point-2, and the algorithm takes a decision at point-2 by considering *dV* and *dP*. As $dV > 0$ and $dP > 0$ at point-2, the algorithm decreases the converter duty ratio. Now, the operative point is moved to point-3. As $dP < 0$ and $dV > 0$ at point-3, the method raises the converter duty ratio, and now, the operative point is moved to point-2. As $dV < 0$ and $dP > 0$ at point-2, it raises the converter duty ratio further, and now, the operating point is moved to point-1. As $dV < 0$ and $dP < 0$ at point-1, the algorithm decreases the converter duty ratio, and now, the operative point is moved to point-2. As discussed, the operating point oscillates between three locations around the MPP.

D. Drift Occurrence in the P&O Technique

During rapid variations in solar irradiation, which happen typically in cloudy seasons, the chances of getting drift problems are high. Usually, the drift occurrence happens at any of the three operating points. A simple drift incident is shown in Fig. 6. It depends on the change in solar irradiation instant in between the perturbation duration. The drifting issue is due to the absence of information in knowing whether the rise in PV power in the module is because of the increase in solar insolation or an increase in perturbation.

As depicted in Fig. 6, assume that the solar insolation is changed at point-1, and at the same instant, the operating point on the characteristic settles at point-4 during the same perturbation duration (tT_p) as that of point-1. As $dV\,(V_4(tT_p) - V_2((t-1)T_p) > 0$ and $dP\,(P_4(tT_p) - P_2((t-1)T_p) > 0$ at point-4, it decreases the converter duty ratio, and the operative point moves away from the MPP, i.e., toward the point-5. Similar to this, the problem due to drift occurs at the point-3 and point-2 as well.

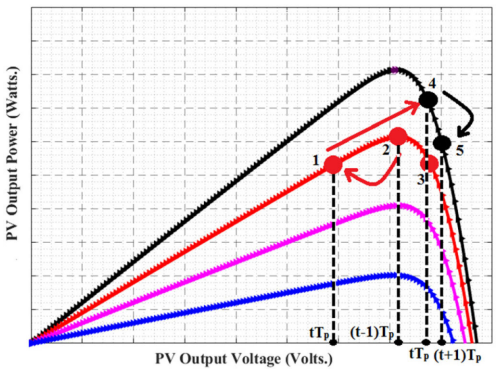

Fig. 6. Drift analysis in traditional P&O under a change in insolation.

The problem due to drift is serious in case of a fast change in solar irradiation.

The steady-state response and tracking time depend on the size of the perturbation. To improve the transient and steady-state response of this method, an adjustable perturbation size is selected [32]. The converter duty ratio is derived as follows:

$$D(t) = D(t-1) \pm M\left(\frac{|dP|}{|dV|}\right). \tag{4}$$

It is observed from (4) that a change in solar insolation increases the perturbation size depending on the magnitude of change in power, *dP*, change in voltage, *dV*, and the scaling factor, *M*. Therefore, the problem due to drift is more in adjustable step size P&O MPPT technique under a change in isolation due to the high perturbation step size [43], [44].

IV. Proposed Enhanced P&O MPPT Technique

The conventional algorithm is established by the values such as *dV* and *dP* on the *P–V* curve of the panel. As discussed in Section III, the problems due to drift are because of confusion by the algorithm, and this can be diminished by adding another parameter called *dI*. The load line slope can express the relationship between $V_{\rm pv}$ and $I_{\rm pv}$ under a change in solar insolation condition. The relationship is given as follows:

$$I_{\rm pv} = \left(\frac{1}{1-D}\right)^2 \times \frac{V_{\rm pv}}{\eta_{\rm Converter} \times R_0}. \tag{5}$$

From the single-diode model, the relation between the voltage and current of the PV module can be presented as follows:

$$I_{\rm pv} = I_{\rm sc} - I_0\left(\exp\left(\frac{V_{\rm pv}}{aV_T}\right) - 1\right) + \frac{V_{\rm pv} + R_{\rm se}I_{\rm pv}}{R_p} \tag{6}$$

where the diode reverse saturation current is I_o, "*a*" is diode ideality factor, $I_{\rm sc}$ is short-circuited current of the PV module, thermal voltage is V_T, R_p is parallel resistance, and $R_{\rm se}$ is the series resistance of the panel. By equating (5) and (6), the expression is derived by applying Taylor's series expansion

$$\left(\frac{1}{1-D}\right)^2 \times \frac{V_{\rm pv}}{\eta_{\rm Converter} \times R_0} = I_{\rm sc} - I_0\left(\frac{V_{\rm pv}}{aV_T}\right) + \frac{V_{\rm pv}}{R_p} - \frac{R_{\rm se}}{R_p} \times \left(\frac{1}{1-D}\right)^2 \times \frac{V_{\rm pv}}{\eta_{\rm Converter} \times R_0}. \tag{7}$$

Simplify (7) and the PV output voltage can be stated in terms of PV output current for the respective solar irradiation, *G*, and load line slope as

$$V_{\rm pv}|\,G = \frac{I_{\rm sc}|\,G}{\frac{1}{(1-D)^2}\left(\frac{1}{\eta_{\rm Converter}\times R_0}\right)\left(1+\frac{R_{\rm se}}{R_p}\right) + \left(\frac{I_0}{aV_T}\right) + \frac{1}{R_p}}. \tag{8}$$

By substituting (8) in (5), (5) is modified as follows:

$$I_{\rm pv}|\,G = \frac{I_{\rm sc}|\,G}{\frac{1}{(1-D)^2}\left(\frac{1}{\eta_{\rm Converter}\times R_0}\right)\left(1+\frac{R_{\rm se}}{R_p}\right) + \left(\frac{I_0}{aV_T}\right) + \frac{1}{R_p}} \times \frac{1}{(1-D)^2}\left(\frac{1}{\eta_{\rm Converter} \times R_0}\right). \tag{9}$$

The short-circuit current at actual irradiation condition, *G*, can be derived concerning $I_{\rm sc}$ at nominal operating conditions. The short-circuit current at *G* is expressed as

$$I_{\rm sc}|\,G = (I_{{\rm sc},n} + K_I \times dT) \times \frac{G}{G_n} \tag{10}$$

where K_I is the temperature coefficient at the short-circuit current, G_n is the solar irradiation under nominal operating condition, and *dT* is equal to the difference between the nominal temperature (T_n) and the actual temperature (*T*).

Substitute (10) in (8) and (9) and by considering the $I_{\rm pv}$ and $V_{\rm pv}$ derivatives concerning solar irradiation, the consequence on $V_{\rm pv}$ and $I_{\rm pv}$ due to changes in insolation can be derived

$$\frac{dV_{\rm pv}}{dG} = \frac{(I_{{\rm sc},n} + K_I \times dT) \times \frac{1}{G_n} + K_I\frac{G}{G_n}\frac{dT}{dG}}{\frac{1}{(1-D)^2}\left(\frac{1}{\eta_{\rm Converter}\times R_0}\right)\left(1+\frac{R_{\rm se}}{R_p}\right) + \left(\frac{I_0}{aV_T}\right) + \frac{1}{R_p}} > 0 \tag{11}$$

$$\frac{dI_{\rm pv}}{dG} = \frac{(I_{{\rm sc},n} + K_I \times dT) \times \frac{1}{G_n} + K_I\frac{G}{G_n}\frac{dT}{dG}}{\frac{1}{(1-D)^2}\left(\frac{1}{\eta_{\rm Converter}\times R_0}\right)\left(1+\frac{R_{\rm se}}{R_p}\right) + \left(\frac{I_0}{aV_T}\right) + \frac{1}{R_p}} \times \frac{1}{(1-D)^2}\left(\frac{1}{\eta_{\rm Converter} \times R_0}\right) > 0. \tag{12}$$

The change in solar irradiation and temperature variation is directly proportional to each other. It is observed from (11) and (12) that the denominator is positive and the numerator is positive since the parameters such as K_I, $I_{{\rm sc},n}$, and *dT/dG* are positive. Thus, the states in (11) and (12) are valid, and hence, it is observed that $V_{\rm pv}$ and $I_{\rm pv}$ increase when the solar insolation increases. It is concluded that the problem due to drift can be avoided by having *dV* and *dI* information.

The operative point variation on the *V–I* curves under the rise in solar irradiation condition is shown in Fig. 7(a). Consider the test case of increase in solar insolation condition, as shown in Fig. 7(a), and notice that the operating point at point-3 is moved to the new operating point at point-4. The proposed algorithm takes a decision at point-3 at which $dI\ (I_2(k-1)T_p - I_4(tT_p)) < 0$ as shown in Fig. 7(a). Simultaneously, the *P–V* characteristic at point-4, $dP\ (P_4(tT_{\rm p}) - P_2((t-1)T_p) > 0$ and $dV\ (V_4(tT_p) - V_2((t-1)T_p) > 0$ as shown in Fig. 7(b). Thus, the values of the parameters such as *dV*, *dI*, and *dP* are positive at point-4. So, the confusion on the positive *dP* value is because of perturbation size or the rise in solar irradiation and is avoided by adding an

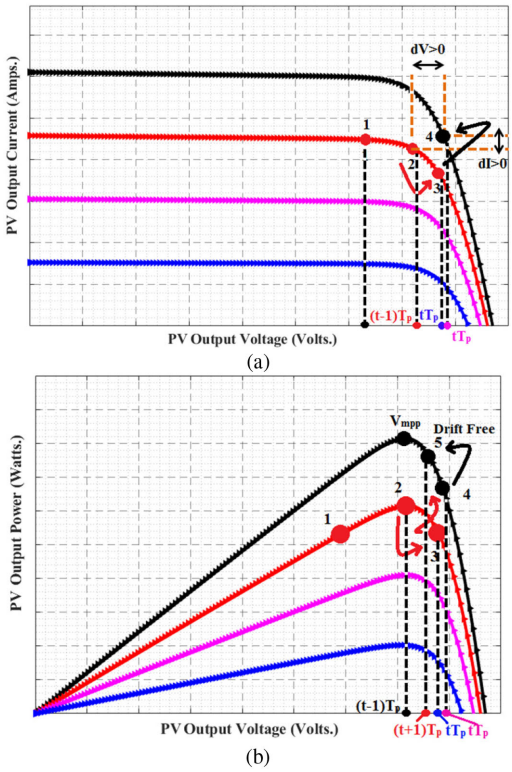

Fig. 7. Observation of drift avoidance in the proposed technique. (a) During a change in current. (b) During an increase in solar insolation.

extra parameter, *dI*. From Fig. 7(a), it is observed that *dI* and *dV* will never have a similar sign for distinct insolation.

The parameters, such as *dI* and *dV*, are positive, and it is applicable only for the rise in solar irradiation, as shown in Fig. 8(a). Therefore, the rise in solar irradiation can be sensed by an extra parameter, *dI*. Thus, the converter duty ratio can be adjusted to reduce the operating voltage, where the values of *dI* and *dV* are positive and can eliminate the issue due to drift by shifting the operating point nearer to MPP. Likewise, for the rise in solar irradiation at the point-2 and point-1, the drift problem can be avoided by adding an extra parameter *dI*. The flow charts for the proposed enhanced P&O technique are displayed in Fig. 8. Fig. 8(a) displays the flow chart for the proposed modified P&O (MP&O) technique with fixed step size (*dD*), and Fig. 8(b) displays the flow chart for the proposed adaptive P&O technique (AMP&O) with variable perturbation size ($M \times dD$), in which, the scaling factor, *M*, varies the perturbation size along with initial step size, *dD*. Thus, the scaling factor, *M*, of the proposed method, is as follows:

$$M = \frac{[V(t+1) - V(t)]}{[P(t+1) - P(t)]} \times \frac{[P(t) - P(t-1)]}{[V(t) - V(t-1)]} = \frac{\Delta V}{\Delta P} \times \frac{dP}{dV}. \tag{13}$$

For guaranteed adequate performance under all operating conditions, it is essential to tune the value of the scaling factor, *M*, automatically during start-up conditions. At the start-up, the value of *dP/dV* is maximum, which will introduce high power oscillations. However, the value of $\Delta V/\Delta P$ is very minimal, which prevents the high value of *dP/dV* subsequently. This consecutively prevents the power oscillations around the maximum

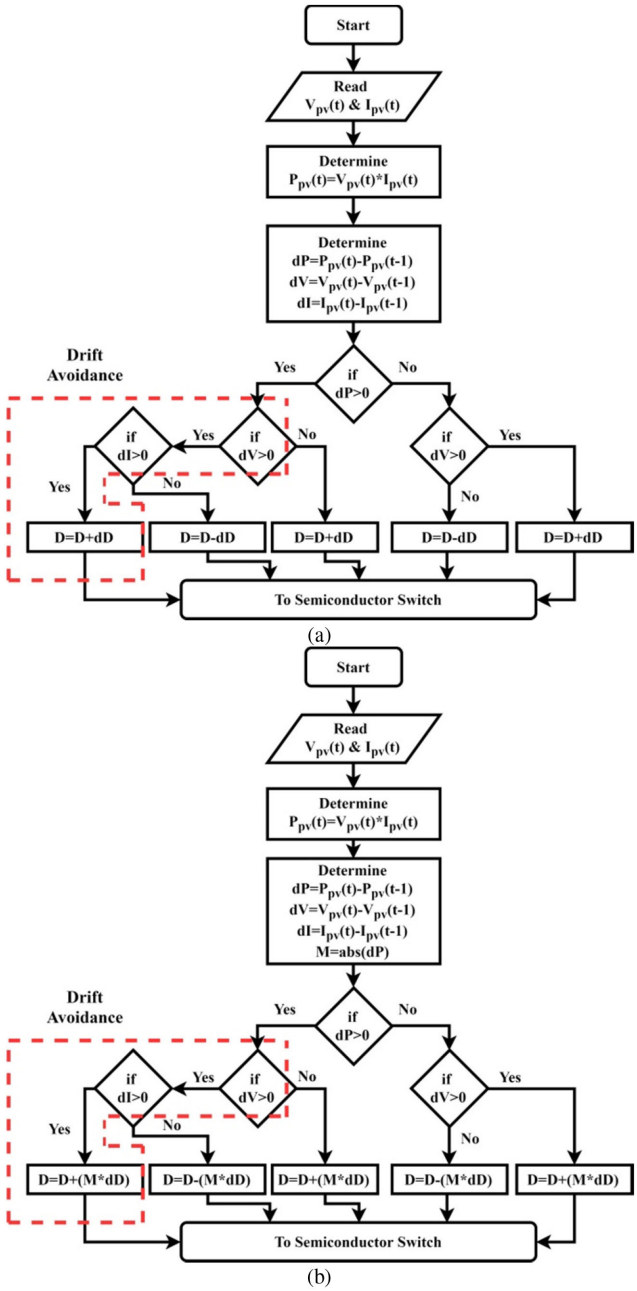

Fig. 8. Flowchart of the proposed techniques. (a) Modified P&O (MP&O) method with constant step size. (b) Adaptive modified P&O (AMPO) method with a variable step size.

operating point during the steady-state operating condition. Besides, the auto-tuning of the scaling factor shows better performance during steady-state and dynamic operating conditions irrespective of the source from the module/string/array. If the scaling factor is manually tuned, the system is susceptible to start-up conditions. If the fixed value of the scaling factor is calculated under certain operating conditions, it leads to instability during other operating conditions. Therefore, the scaling factor is always automatically tuned as per (13) to get better results.

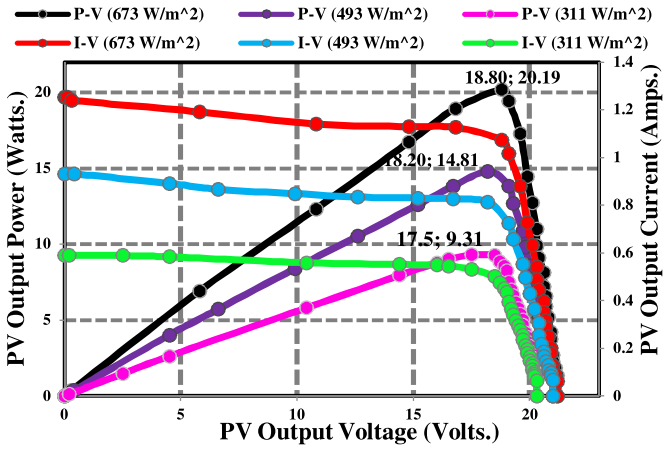

Fig. 9. *I–V* and *P–V* curves under step change in insolation (experimental data).

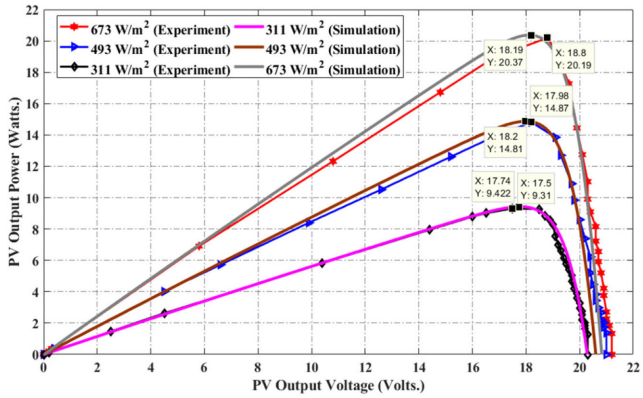

Fig. 10. *P–V* characteristics during simulation and experimentation under step change in irradiation.

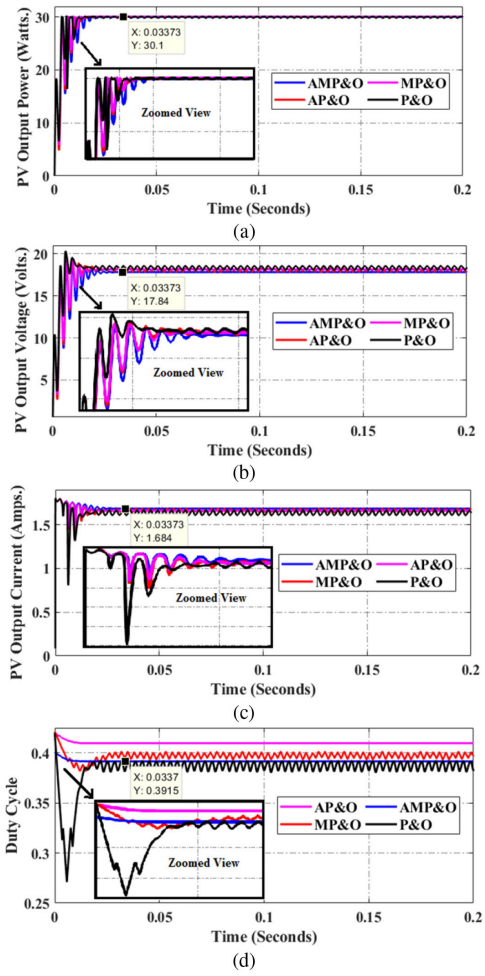

Fig. 11. Simulation waveforms under STCs. (a) PV power. (b) PV voltage. (c) PV current. (d) Duty cycle.

V. Numerical Simulation Results

To assess the proposed MPPT technique, the simulations have been carried out using Matlab/Simulink software. To proceed further, as a PV source, the single-diode PV model is considered with the module parameters such as $I_o = 23.08 \times 10^{-8}$ A, $a = 1.3$, $I_{\mathrm{pv},n} = 1.9$ A, $R_{\mathrm{se}} = 0.137\,\Omega$, and $R_p = 208\,\Omega$ at nominal operating conditions. As a power interface between the PV array and the load, the dc–dc boost converter has been designed, and its parameters are given as follows: inductance, $L = 1.2$ mH, switching frequency, $f_s = 20$ kHz, input and output capacitors, $\mathrm{C_{in}} = \mathrm{C_{out}} = 220\ \mu$F, and the load resistance, $R_L = 30\,\Omega$. *I–V* and *P–V* curves of the module during experimentation under various solar insolation condition is shown in Fig. 9.

The PV characteristics during simulation and experimentation are plotted and displayed in Fig. 10. It is observed that the PV output voltages at MPP are 18.19, 18.2, and 17.74 V (during simulation), 18.8, 18.2, and 17.5 V (during experimentation), and the corresponding solar irradiation levels are 673.04, 493.1, and 310.83 W/m^2, respectively. The simulation and experimentations have been performed under various cases, such as standard test condition (STC), one-step change in solar insolation, and a rapid change in solar insolation.

In addition, the proposed algorithms are compared with other algorithms in the literature. It is not appropriate to compare the proposed algorithms with bio-inspired or soft computing based MPPT methods. Therefore, the proposed algorithms are only compared with the traditional P&O MPPT method and adaptive P&O MPPT method discussed in the literature to avoid confusion among the readers.

A. Simulation Under Standard Test Conditions (STC)

The effectiveness of the proposed modified P&O (MP&O) and an adaptive modified P&O (AMP&O) MPPT algorithm is simulated under STCs, i.e., the temperature, T is 25 °C, and the solar insolation, G is 1000 W/m^2. The comparison is made between the conventional P&O technique and an adaptive P&O (AP&O) along with the proposed MPPT methods. The waveforms are depicted in Fig. 11.

It is observed from the results that all the algorithms are capable of tracking the maximum power (30.12 W) accurately within 0.039 s. During steady state, the conventional P&O algorithm produces oscillations due to the improper selection of the step size. For the simulation analysis, the perturbation time (T_p) and size (dD) are selected as 10 ms and 1.5%, respectively. It is observed that techniques such as AP&O and AMP&O produce

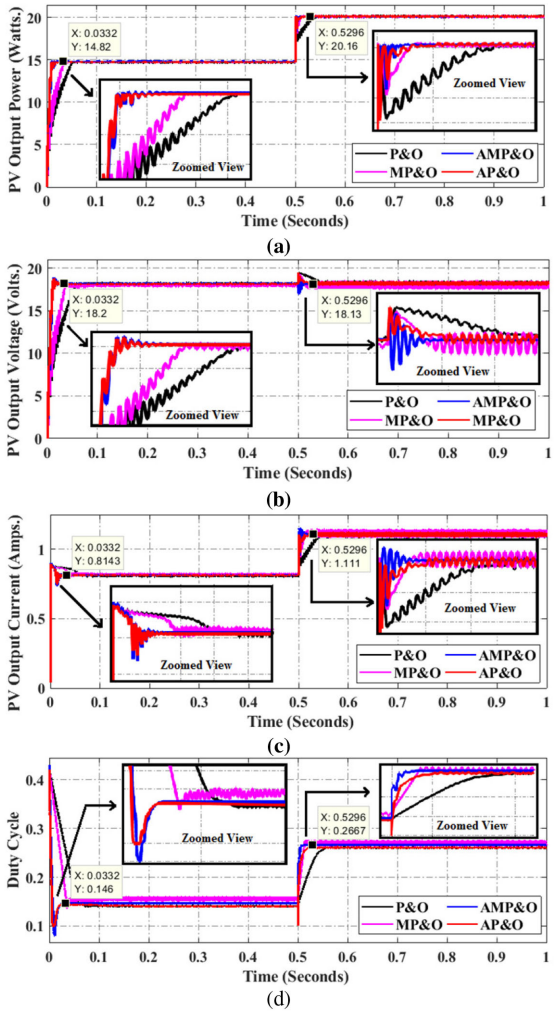

Fig. 12. Simulation waveforms under one-step change in irradiation. (a) PV power. (b) PV voltage. (c) PV current. (d) Duty cycle.

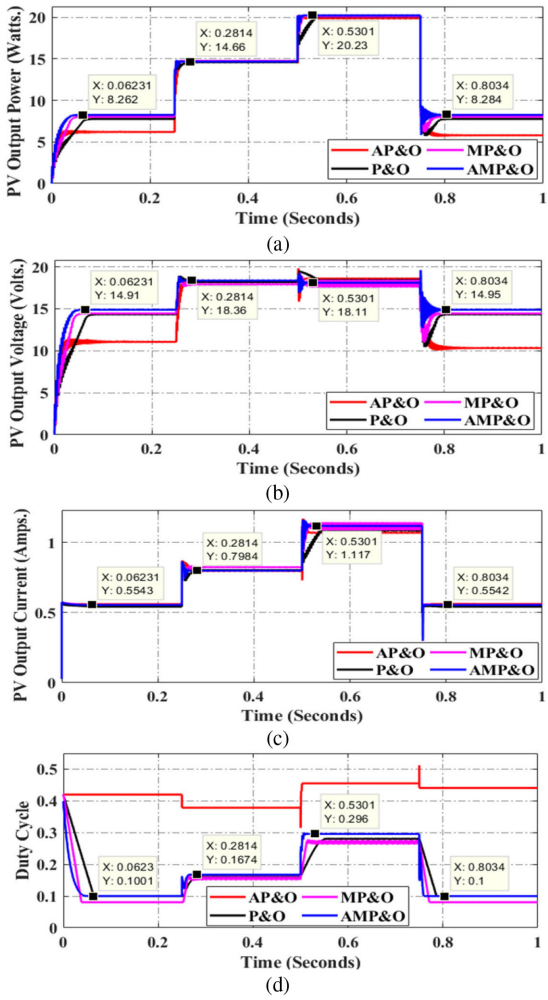

Fig. 13. Simulation waveforms under rapid change in irradiation. (a) PV power. (b) PV voltage. (c) PV current. (d) Duty cycle.

zero oscillation during steady state, and MP&O produces very fewer oscillations.

However, the tracking time of the AMP&O method is about 0.03373 s and the MP&O technique is 0.03412 s., which is less than the conventional AP&O and P&O methods. It is visible from Fig. 11 that the conventional P&O technique is affected by the sizeable steady-state oscillation, and the same can be diminished by choosing a shallow step size, which further increases the tracking time.

B. Simulation Under a One-Step Change in Irradiation

The effectiveness of the proposed MP&O and AMP&O algorithms is simulated under a one-step change in irradiation, i.e., G is initially kept at 493 W/m^2 and altered to 673 W/m^2 at 0.5 s. With $T = 38$ °C. The comparison is made between the conventional P&O and AP&O, along with the proposed MPPT methods. The obtained simulation waveforms under this test case are depicted in Fig. 12.

For the simulation under this test case, the perturbation size (dD) is selected as 1.5% for the proposed techniques, whereas for other MPPT techniques, the step size is selected as 4.5% to avoid the drift. Because of the large step size, the drift condition is avoided in conventional MPPT techniques; however, the proposed methods are unaffected with the same step size as similar to the STC case. Due to this, the tracking time is very less for proposed methods, as seen in Fig. 12(a) with almost zero drift. The time taken by the proposed AMP&O method to track the MPP (14.82 W, 18.2 V, 0.8143 A) at 493 W/m^2 is 0.0332 s and time to track the MPP (20.16 W, 18.13 V, 1.11 A) at 673 W/m^2 is 0.0296 s. From Fig. 12(a)–(d), it is observed that the techniques proposed in this article are capable of tracking the MPP with less tracking time and almost zero steady-state oscillations.

C. Simulation Under a Rapid Increase in Irradiation

During cloudy days, solar insolation changes rapidly, which will affect the performance of the PV system. Therefore, to validate the performance of proposed methods, a test case called a rapid change in insolation is also considered. So, the proposed algorithms are simulated under a rapid increase in irradiation, i.e., G is initially kept at 311 W/m^2, changed to 493, 673, and 311 W/m^2 after every 0.25 s, with $T = 38$ °C. The comparison waveforms are shown in Fig. 13 for various techniques. The issue due to drift is substantial during a rapid change in irradiation conditions. The effectiveness of the proposed techniques is

TABLE III
COMPARISON OF PROPOSED MPPT METHODS WITH OTHER MPPT TECHNIQUES

Parameters	P&O	AP&O	MP&O	AMP&O
Power loss	Very High	High	Medium	Low
Steady-state oscillation @ rapid rise in G	Very High	High	Medium	Low
Drift possibility	Very High	High	Medium	Zero
Tracking time	High	Medium	Medium	Low
Tracking accuracy	Low	Medium	Medium	High
Perturbation size (dD)	5%	4%	2%	2%
Implementation complexity	Low	Medium	Low	Medium

compared with respect to conventional MPPT techniques. The simulation is performed for a rapid rise in solar irradiation from 311 to 673 W/m^2 and brought back to 311 W/m^2. The insolation change is performed at 0.25 s, each. In the conventional algorithms, the drift conditions are avoided by selecting the large perturbation size. From Fig. 13, it is observed that the conventional P&O be able to reduce the drift with a large step size (>5%). However, the power loss is high because of the presence of power oscillations around the MPP. The AP&O fails to trace the MPP because step size variation depends on the *dP*. The power loss is more in AP&O during a rapid rise in irradiation.

The proposed methods, such as MP&O and AMP&O, are capable of tracking the MPP without further power oscillations with less tracking time. The time taken by the proposed AMP&O method to track the MPP (8.262 W, 14.91 V, 0.5543 A) at 311 W/m^2 is 0.06231 s, (14.66 W, 18.36 V, 0.7984 A) at 493 W/m^2 is 0.0314 s, the time to track the MPP (20.23 W, 18.11 V, 1.17 A) at 673 W/m^2 is 0.0301 s, and (8.284 W, 14.95 V, 0.5534 A) at 311 W/m^2 is 0.0534 s. It is worth to mention from Fig. 13 that the tracking is done in proposed techniques without changing the perturbation size during a rapid increase in insolation. The power loss (P_{loss}) during steady state is calculated concerning maximum available power based on

$$\frac{P_{\text{loss}}}{P_{\text{mp}}} = \left(\frac{dV_{\text{pv,RMS}}}{V_{\text{mp}}}\right) - \left(1 + \frac{V_{\text{mp}}}{2aV_T}\right) \tag{14}$$

where the RMS steady-state output voltage oscillation is $dV_{\text{pv, RMS}}$, and V_{mp} is the maximum output voltage at MPP. From (14) and Fig. 13(a), it is noticed that the power loss is high with AP&O and P&O techniques because of significant voltage oscillations. The comparison between different MPPT techniques is given in Table III.

VI. EXPERIMENTAL RESULTS AND FURTHER DISCUSSIONS

The experimental validation of the proposed techniques is carried out on the conventional boost converter. The experimental setup has been built by considering the same parameters, which are presented in Section V of this article. The pulse width modulated (PWM) gate signal for the boost converter is generated using MSP430G2553 Texas Instruments mixed-signal-processor for the digital implementation of the algorithm. The photograph of the developed experimental setup is presented in Fig. 14.

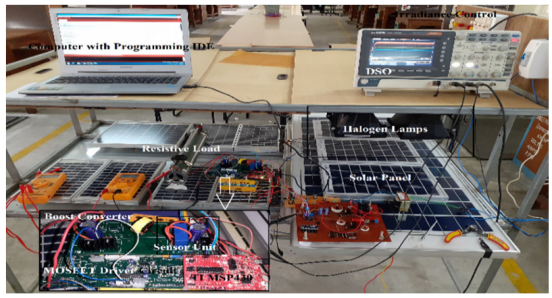

Fig. 14. Experimental setup of the solar PV MPPT system.

Since the working of the proposed techniques is based on the inputs from the voltage sensor and current sensor, the sensors with high accuracy are must to implement these methods. The PV module voltage is sensed by a simple voltage divider network with the resistance R_1 and R_2 of the values 2 and 10 kΩ, respectively. The PV panel current is sensed by LEM LA 55-P, a hall effect-based current sensor. The PV module having model number EFS12010MC36 is selected for experimental validation. The solar insolation is generated artificially by 500 W halogen lamps in a constant temperature environment. The solar insolation is artificially varied using electronic voltage regulators. The regulator is fixed at three different operating points to get the different insolation levels, for instance, 673, 493, and 311 W/m^2 at 35 °C temperature.

A. Case 1: Constant Solar Insolation Condition

The different MPPT techniques with the step size, as presented in Table III, is verified for constant solar insolation at 673 W/m^2. The experimental waveforms are shown in Fig. 15. Fig. 15(a) gives the PV voltage, PV current, and PV power for the proposed AMP&O technique.

From Fig. 15(a)–(b), it is observed that the proposed methods, such as AMP&O and MP&O, can track the same maximum output of 16.74 W at 18.6 V and 0.9 A. On the other hand, the conventional P&O method can track the power of 13.94 W at 17.0 V, and 0.82 A with large power oscillation due to the large step size of 5% and the same can be witnessed from Fig. 15(c). However, the traditional AP&O can track the maximum output power of 17.67 W at 19 V and 0.93 A with high tracking time, as illustrated in Fig. 15(d). It can be observed that there is a large power oscillation due to the variable step size. The output power oscillates between 15.664 and 17.67 W.

B. Case 2: One Step Change in Solar Insolation

The effectiveness of the algorithms is also confirmed under a one-step change in solar insolation conditions and compared with the conventional algorithms. The insolation is changed from 673 to 311 W/m^2 after 0.5 s. Fig. 16 displays the experimental waveforms for a one-step change in insolation condition.

Fig. 16(a) indicates the PV voltage, PV current, and PV power for the proposed AMP&O technique. From Fig. 16(a) and (b), it is observed that the proposed methods, such as AMP&O and MP&O, are capable of tracking the highest output power of 8.62 W at 311 W/m^2 and the AMP&O algorithm can track the maximum output power of 16.4 W, whereas the MP&O can track 16.21 W at 673 W/m^2. On the other hand, the conventional P&O

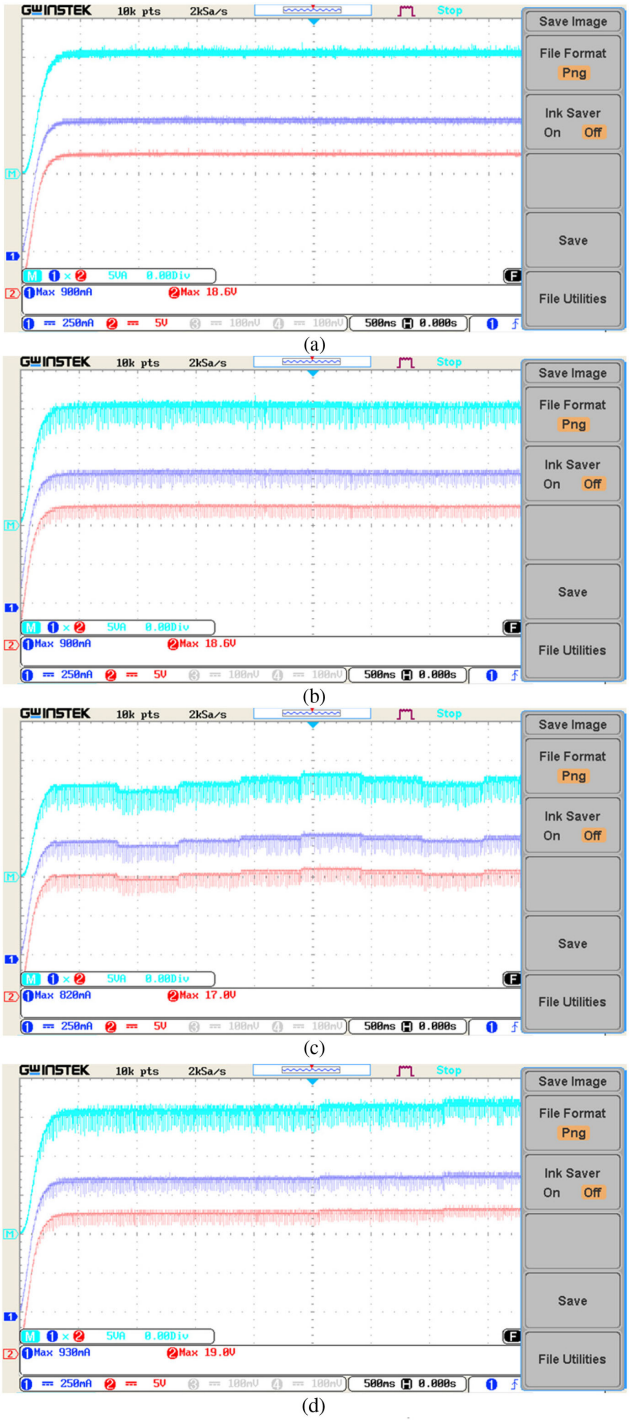

Fig. 15. Experimental waveforms at 673 W/m^2 at 35 °C. (a) AMP&O. (b) MP&O. (c) P&O. (d) AP&O.

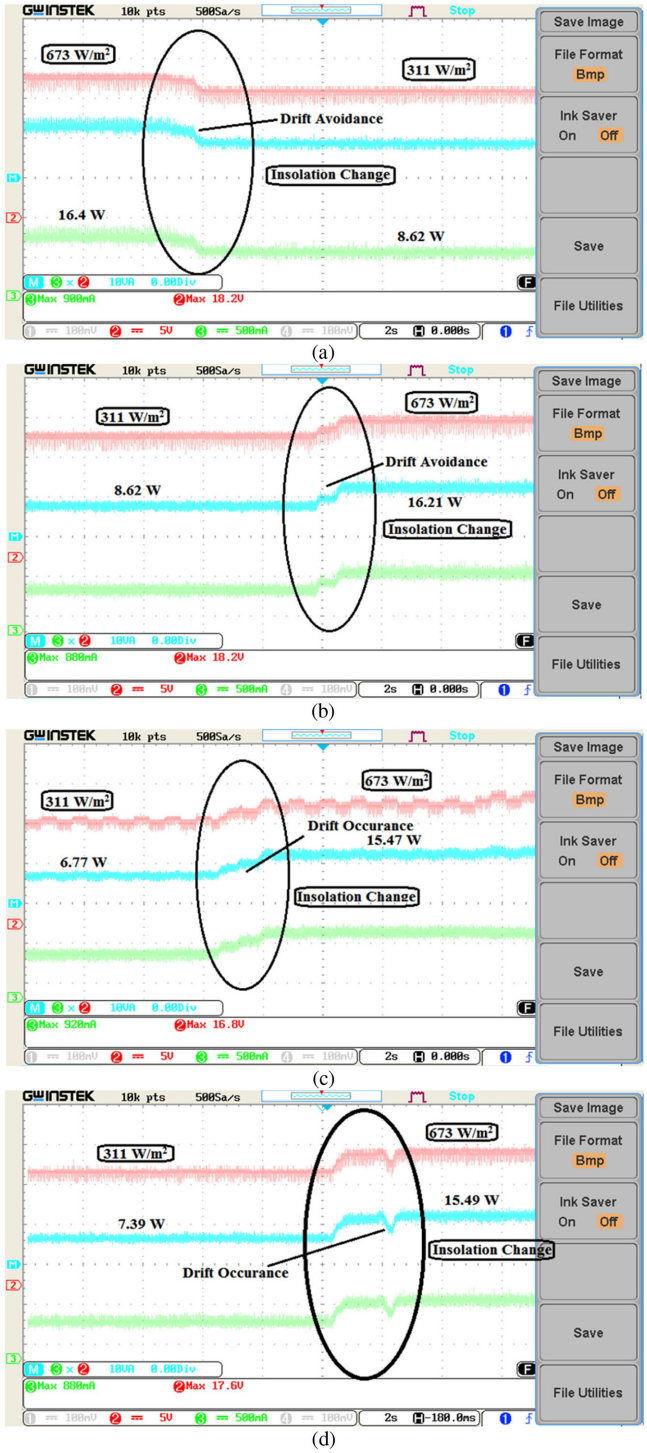

Fig. 16. Experimental waveforms for one-step change in insolation condition at 35 °C. (a) AMP&O. (b) MP&O. (c) P&O. (d) AP&O.

method can track the power of 6.77 W with power oscillations due to the large step size of 5% at 311 W/m^2 and AP&O can track 7.39 W. The drift has occurred in both P&O and AP&O algorithms when the solar irradiation is changed from 311 to 673 W/m^2, and the same has been observed in Fig. 16(c) and (d). It is observed that, for step-change in irradiation, the output voltage is enlarged, and it results in the conventional algorithms to stay away from the MPP. The drift condition is avoided in MP&O and AMP&O techniques, and these techniques are capable of tracking the MPP accurately without power oscillations with less tracking time.

C. Case 3: Rapid Change in Solar Insolation

The effectiveness of the algorithms is also validated under a rapid change in solar irradiation conditions. The insolation is

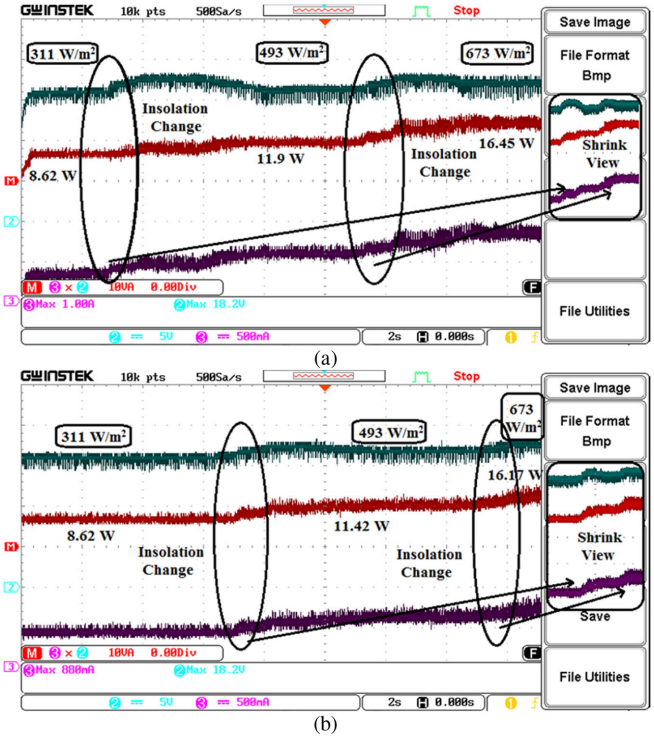

Fig. 17. Experimental waveforms for rapid change in insolation at 35 °C. (a) AMP&O. (b) MP&O.

TABLE IV
COMPARISON OF THE PROPOSED ALGORITHMS UNDER A RAPID CHANGE IN INSOLATION CONDITIONS

Parameters	Conventional P&O	[29]	[34]	Proposed methods
Response time (s)	3.8	2.2	1.8	0.8 (AMP&O) 1.1 (MP&O)
Power oscillation ratio	35 %	20 %	20 %	10% (AMP&O) 15 % (MP&O)
Tracking time (s)	0.08215	0.0525	0.0611	0.0337 (AMP&O) 0.03412 (MP&O)
Average Tracking efficiency	< 92 %	≤ 95%	≤ 95%	≥ 95%

changed from 311 W/m^2 to 493 W/m^2 and 673 W/m^2 after 0.5 s. Fig. 17 shows the experimental waveforms for rapid change in insolation conditions.

Fig. 17(a) represents the PV voltage, PV current, and PV power for the proposed AMP&O technique. From Fig. 17(a), it is noticed that the AMP&O can track the maximum power of 8.62 W (17.8 V, 0.484 A) at 311 W/m^2, 11.9 W (17.7 V, 0.672 A) at 493 W/m^2, and 16.45 W (18.1 V, 0.91 A) at 673 W/m^2. From Fig. 17(b), it is noticed that the proposed MP&O can track the maximum power of 8.62 W (17.9 V, 0.481 A) at 311 W/m^2, 11.42 W (17.7 V, 0.642 A) at 493 W/m^2, and 16.17 W (18.2 V, 0.888 A) at 673 W/m^2. The drift condition is almost avoided in both MP&O and AMP&O techniques, and these techniques are capable of tracking the MPP accurately without power fluctuations with less tracking time. It is noticed that, for rapid change in irradiation, the output voltage is reduced, and the output power is enlarged. This situation causes the proposed algorithms to move near the MPP and track the MPP accurately than the conventional algorithms.

To show an excellency of the proposed method, in addition to the tracking power and reducing oscillations, a few other essential findings of the proposed method are presented in Table IV. It is clearly observed from Table IV that the proposed MPPT methods significantly increase the performance in steady-state (70% of power oscillation reduction) as well as dynamic condition (less convergence time) increasing by way of power transfer.

To conclude the study, the AMP&O and MP&O algorithms based MPPT techniques are capable of working effectively toward a constant insolation condition and various changes in insolation conditions with a high tracking efficiency and less tracking time. It is concluded that, throughout the 25-years life span of the PV module, a significant energy gain may be achieved due to the proposed MPPT methods for the PV plants.

VII. CONCLUSION

This article investigates and outlines the problem in the traditional P&O MPPT technique and presents new MPPT techniques called MP&O and AMP&O, which can significantly reduce the computational problem. The drift-free condition is achieved by including the change in current, *dI*, profile with the existing change in voltage, *dV*, and power, *dP* profile. The mathematical analysis justifies the advantage of the proposed techniques. Both simulation and experimentation validate the effectiveness of the algorithms under different operating scenarios. The experimental and simulation results demonstrate that the AMP&O and MP&O techniques can avoid the issue called drift, and it tracks the MPP accurately with less tracking time and responds faster than the other techniques. The proposed techniques can deliver tracking efficiency of above 95% under various scenarios due to drift-free operating conditions. The proposed methods are more suitable for low-cost implementation of the PV system due to its simplicity and robustness. On the other hand, the bio-inspired algorithms based methods involve huge implementation cost along with the high computational complexity. The future extension will be concentrated on the reliability of the MPPT algorithms when both temperature and shading are taken into consideration. The techniques may be employed for solar PV-based water pumping systems in the agricultural field due to its cost-effective solution.

REFERENCES

[1] A. Jafari, T. Khalili, H. Ganjeh Ganjehlou, and A. Bidram, "Optimal integration of renewable energy sources, diesel generators, and demand response program from pollution, financial, and reliability viewpoints: A multi-objective approach," *J. Clean. Prod.*, vol. 247, Feb. 2020, Art. no. 119100.

[2] P. Bhatnagar and R. K. Nema, "Maximum power point tracking control techniques: State-of-the-art in photovoltaic applications," *Renewable Sustain. Energy Rev.*, vol. 23, pp. 224–241, Jul. 2013.

[3] M. Premkumar, K. Karthick, and R. Sowmya, "A comparative study and analysis on conventional solar PV based DC-DC converters and MPPT techniques," *Indo. J. Elect. Eng. Comput. Sci.*, vol. 11, no. 3, pp. 831–838, Sep. 2018.

[4] M. Premkumar and R. Sowmya, "Certain study on MPPT algorithms to track the global MPP under partial shading on solar PV module/array," *Int. J. Comput. Digit. Syst.*, vol. 8, no. 4, pp. 405–416, Jul. 2019.

[5] Q. Mei, M. Shan, L. Liu, and J. M. Guerrero, "A novel improved variable step-size incremental-resistance MPPT method for PV systems," *IEEE Trans. Ind. Electron.*, vol. 58, no. 6, pp. 2427–2434, Jun. 2011.

[6] M. Premkumar and T. R. Sumithira, "Design and implementation of new topology for non-isolated DC-DC micro converter with effective clamping circuit," *J. Circuits, Syst. Comput.*, vol. 28, no. 5, May 2019, Art. no. 1950082.

[7] W. Xiao and W.G. Dunford, "A modified adaptive hill climbing MPPT method for photovoltaic power systems," in *Proc. IEEE Annu. Power Electron. Specialists Conf.*, 2004, pp. 1957–1963.

[8] J. Ahmad, "A fractional open circuit voltage based maximum power point tracker for photovoltaic arrays," in *Proc. Int. Conf. Softw. Technol. Eng.*, 2010, pp. V1-247–V1-250.

[9] A. El Khateb, N. A. Rahim, J. Selvaraj, and M. N. Uddin, "Fuzzy logic controller based sepic converter for maximum power point tracking," *IEEE Trans. Ind Appl.*, vol. 50, no. 4, pp. 2349–2358, Aug. 2014.

[10] S. Mohanty, B. Subudhi, and P. K. Rey, "A new MPPT using GWO technique for photovoltaic system under partial shading conditions," *IEEE Trans. Sustain. Energy*, vol. 7, no. 1, pp. 181–188, Jan. 2016.

[11] S. Lyden and Md. Enamul-Haque, "A simulated annealing global maximum power point tracking approach for PV modules under partial shading conditions," *IEEE Trans. Power. Electron.*, vol. 31, no. 6, pp. 4171–4181, Jun. 2016.

[12] J. Ahmed and Z. Salam, "A maximum power point tracking for PV system using Cuckoo Search with partial shading capability," *Appl. Energy*, vol. 119, pp. 119–129, Apr. 2014.

[13] B. Peng, K. Ho, and Y. Liu, "A novel and fast MPPT method suitable for both fast changing and partially shaded conditions," *IEEE Trans. Ind. Electron.*, vol. 65, no. 4, pp. 3240–3251, Apr. 2018.

[14] S. Titri, C. Larbes, K. Y. Toumi, and K. Benatchba, "A new MPPT controller based on the Ant colony optimization algorithm for photovoltaic systems under partial shading conditions," *Appl. Soft Comput.*, vol. 58, pp. 465–479, Sep. 2017.

[15] Y. H. Liu, S. C. Huang, W. Huang, and W. C. Liang, "A particle swarm optimization based maximum power point tracking algorithm for PV systems operating under partially shaded conditions," *IEEE Trans. Energy Convers.*, vol. 27, no. 4, pp. 1027–1035, Dec. 2012.

[16] H. Li, D. Yang, W. Su, J. Lü, and X. Yu, "An overall distribution particle swarm optimization MPPT algorithm for photovoltaic system under partial shading," *IEEE Trans. Ind. Electron.*, vol. 66, no. 1, pp. 265–275, Jan. 2019.

[17] A. S. Benyoucef, A. Chouder, K. Kara, S. Silvestre, and O. A. Sahed, "Artificial bee colony-based algorithm for maximum power point tracking (MPPT) for PV systems operating under partial shaded conditions," *Appl. Soft Comput.*, vol. 32, pp. 38–48, 2015.

[18] S. Hosseini, S. Taheri, M. Farzaneh, and H. Taheri, "A high-performance shade-tolerant MPPT based on current-mode control," *IEEE Trans. Power Electron.*, vol. 34, no. 10, pp. 10 327–10 340, Oct. 2019.

[19] T. Khalili, S. Nojavan, and K. Zare, "Optimal performance of microgrid in the presence of demand response exchange: A stochastic multi-objective model," *Comput. Elect. Eng.*, vol. 74, pp. 429–450, Mar. 2019.

[20] K. L. Lian, J. H. Jhang, and I. S. Tian, "Maximum power point tracking method based on perturb-and-observe combined with particle swarm optimization," *IEEE J. Photovolt.*, pp. 626–633, Jan. 2014.

[21] A. Harrag and S. Messalti, "PSO-based SMC variable step size P&O MPPT controller for PV systems under fast changing atmospheric conditions," *Int. J. Numer. Model.: Electron. Netw., Devices Fields*, vol. 32, pp. 1–24, May 2019, Art no. e2603.

[22] M. Premkumar and T. R. Sumithira, "Humpback whale assisted hybrid maximum power point tracking algorithm for partially shaded solar photovoltaic systems," *J. Power Electron.*, vol. 18, no. 6, pp. 1805–1818, Dec. 2018.

[23] Y. Dalia, T. Sudhakar Babu, D. Allam, V. K. Ramachandaramurthy, and M. B. Etiba, "A novel chaotic flower pollination algorithm for global maximum power point tracking for photovoltaic system under partial shading conditions," *IEEE Access*, vol. 7, pp. 1 21 432–1 21 445, Aug. 2019.

[24] Y. Dalia, T. Sudhakar Babu, D. Allam, V. K. Ramachandaramurthy, E. Beshr, and M. Eteiba, "Fractional chaos maps with flower pollination algorithm for partial shading mitigation of photovoltaic systems," *Energies*, vol. 12, no. 18, Sep. 2019, Art. no. 3548.

[25] H. M. El-Helw, A. Magdy, and M. I. Marei, "A hybrid maximum power point tracking technique for partially shaded photovoltaic arrays," *IEEE Access*, vol. 5, pp. 11900–11908, Jun. 2017.

[26] A. Jafari, T. Khalili, E. Babaei, and A. Bidram, "A hybrid optimization technique using exchange market and genetic algorithms," *IEEE Access*, vol. 8, pp. 2417–2427, Jan. 2020.

[27] N. Priyadarshi, S. Padmanaban, J. B. Holm-Nielsen, F. Blaabjerg, and M. S. Bhaskar, "An experimental estimation of hybrid ANFIS–PSO-based MPPT for PV grid integration under fluctuating sun irradiance," *IEEE Syst. J.*, vol. 14, no. 1, pp. 1218–1229, Mar. 2020.

[28] M. A. Algendy, B. Zahawi, and D. J. Atkinson, "Assessment of perturb and observe MPPT algorithm implementation techniques for PV pumping applications," *IEEE Trans. Sustain. Energy*, vol. 3, no. 1, pp. 21–33, Jan. 2012.

[29] Y. Yang and H. Wen, "Adaptive P&O MPPT with current predictive and decoupled power control for grid-connected photovoltaic inverters," *J. Modern Power Syst. Clean Energy*, vol. 7, no. 2, pp. 422–432, Mar. 2019.

[30] J. Ahmed and Z. Salam, "An enhanced adaptive P&O MPPT for fast and efficient tracking under varying environmental conditions," *IEEE Trans. Sustain. Energy*, vol. 9, no. 3, pp. 1487–1496, Jan. 2018.

[31] S. K. Kollimalla and M. K. Mishra, "Variable perturbation size adaptive P&O MPPT algorithm for sudden changes in irradiance," *IEEE Trans. Sustain. Energy*, vol. 5, no. 3, pp. 718–728, Jul. 2014.

[32] N. Femia, D. Granozio, G. Petrone, G. Spagnuolo, and M. Vitelli, "Predictive and adaptive MPPT perturb and observe method," *IEEE Trans. Aerosp. Electron. Syst.*, vol. 43, no. 3, pp. 934–950, Nov. 2007.

[33] A. Pandey, N. Dasgupta, and A. K. Mukerjee, "High-performance algorithms for drift avoidance and fast tracking in solar MPPT system," *IEEE Trans. Energy. Convers.*, vol. 23, no. 2, pp. 681–689, Apr. 2008.

[34] R. Alik and A. Jusoh, "An enhanced P&O checking algorithm MPPT for high tracking efficiency of partially shaded PV module," *Sol. Energy*, vol. 163, pp. 570–580, Jan. 2018.

[35] J. Ahmed and Z. Salam, "A modified P&O maximum power point tracking method with reduced steady-state oscillation and improved tracking efficiency," *IEEE Trans. Sustain. Energy*, vol. 7, no. 4, pp. 1506–1515, Oct. 2016.

[36] K. Sangeetha, T. Sudhakar Babu, N. Sudhakar, and N. Rajasekar, "Modeling, analysis and design of efficient maximum power extraction method for solar PV system," *Sustain. Energy Technol. Assess.*, vol. 15, pp. 60–70, Jul. 2016.

[37] T. Sudhakar Babu, K. Sangeetha, and N. Rajasekar, "Voltage band based improved particle swarm optimization technique for maximum power point tracking in solar photovoltaic system," *J. Renewable Sustain. Energy*, vol. 8, no. 1, Jan. 2016, Art. no. 013106.

[38] M. Premkumar, T. R. Sumithira, and R. Sowmya, "Modelling and implementation of cascaded multilevel inverter as solar PV based microinverter using FPGA," *Int. J. Intell. Eng. Syst.*, vol. 11, no. 2, pp. 18–27, Apr. 2018.

[39] M. Premkumar, C. Kumar, and R. Sowmya, "Mathematical modelling of solar photovoltaic cell/panel/array based on the physical parameters from the manufacturer's datasheet," *Int. J. Renewable Energy Develop.*, vol. 9, no. 1, pp. 7–22, Mar. 2020.

[40] S. K. Bhavneshkumar and J. H. Tarunkumar, "Review of maximum power point tracking techniques for photovoltaic arrays working under uniform/non-uniform insolation level," *Int. J. Renew. Energy Tech.*, vol. 9, no. 4, pp. 439–452, Oct. 2018.

[41] M. Saad, G. Abdelaziz El, S. Souad, and D. Aziz, "Modeling of photovoltaic system with modified incremental conductance algorithm for fast changes of irradiance," *Int. J. Photoenergy*, vol. 2018, pp. 1–13, Mar. 2018.

[42] L. Abdelhamid, M. Sabir, and H. Abdelghani, "Design, simulation, and hardware implementation of novel optimum operating point tracker of PV system using adaptive step size," *Int. J. Adv. Manuf. Technol.* vol. 101, pp. 1671–1680, Apr. 2019.

[43] G. Rabiaa, B. Houda, and H. Othman, "Developed and STM implementation of modified P&O MPPT technique for a PV system over sun," *EPE J.*, vol. 29, no. 3, pp. 99–119, Nov. 2019.

[44] T. Billel, K. Fateh, R. Toufik, L. Abdelbaset, and F. Hamza, "Design and hardware validation of modified P&O algorithm by fuzzy logic approach based on model predictive control for MPPT of PV systems," *J. Renewable Sustain. Energy*, vol. 9, Aug. 2017, Art. no. 043503.